HHS Public Access

Author manuscript

Int J Comput Assist Radiol Surg. Author manuscript; available in PMC 2021 August 19.

Published in final edited form as:

Int J Comput Assist Radiol Surg. 2009 September ; 4(5): 457–462. doi:10.1007/s11548-009-0356-4.

Comparison of diagnostic quality and accuracy in color-coded versus gray-scale DCE-MR imaging display

A. Mehndiratta,
Department of Radiology E 010, German Cancer Research Center (DKFZ), INF 280, 69120 Heidelberg, Germany

School of Medical Science and Technology, Indian Institute of Technology (IIT), Kharagpur, India

M. V. Knopp,
Department of Radiology, The Ohio State University, Columbus, USA

C. M. Zechmann,
Department of Radiology E 010, German Cancer Research Center (DKFZ), INF 280, 69120 Heidelberg, Germany

M. Owsijewitsch,
Department of Radiology E 010, German Cancer Research Center (DKFZ), INF 280, 69120 Heidelberg, Germany

H. von Tengg-Kobligk,
Department of Radiology E 010, German Cancer Research Center (DKFZ), INF 280, 69120 Heidelberg, Germany

P. Zamecnik,
Department of Radiology E 010, German Cancer Research Center (DKFZ), INF 280, 69120 Heidelberg, Germany

H. U. Kauczor,
Department of Radiology E 010, German Cancer Research Center (DKFZ), INF 280, 69120 Heidelberg, Germany

P. L. Choyke,
Clinical Center, National Institutes of Health, Bethesda, USA

F. L. Giesel
Department of Radiology E 010, German Cancer Research Center (DKFZ), INF 280, 69120 Heidelberg, Germany

Clinical Center, National Institutes of Health, Bethesda, USA

Abstract

dramit.mehndiratta@gmail.com .

Purpose—The purpose of this study was to evaluate the diagnostic value and tumor-vascular display properties (microcirculation) of two different functional MRI post-processing and display (color and gray-scale display) techniques used in oncology.

Materials and methods—The study protocol was approved by the IRB and written informed consent was obtained from all patients. 38 dynamic contrast enhanced magnetic resonance imaging (DCE-MRI) data sets of patients with malignant pleural-mesothelioma were acquired and post-processed. DCE-MRI was performed at 1.5 tesla with a T1-weighted 2D gradient-echo-sequence (TR 7.0 ms, TE 3.9 ms, 15 axial slices, 22 sequential repetitions), prior and during chemotherapy. Subtracting first image of contrast-enhanced-dynamic series from the last, produced gray-scale images. Color images were produced using a pharmacokinetic two-compartment model. Eight raters, blinded to diagnosis, by visual assessment of post-processed images evaluated both diagnostic quality of the images and vasculature of the tumor using a rating scale ranging from −5 to +5. The scores for vasculature were assessed by correlating with the maximum amplitude of the total-tumor-ROI for accuracy.

Results—Color coded images were rated as significantly higher in diagnostic quality and tumor vascular score than gray-scale images ($p < 0.001$, 0.005). ROI signal amplitude analysis and vascular ratings on color coded images were better correlated compared to gray-scale images rating ($p < 0.05$).

Conclusion—Color coded images were shown to have higher diagnostic quality and accuracy with respect to tumor vasculature in DCE-MRI, therefore their implementation in clinical assessment and follow-up should be considered for wider application.

Keywords

DCE-MRI; Color-coded display; Gray-scale display; Angiogenesis; Tumor vasculature

Introduction

With the advancement of post processing tools and computer assistance, diagnostic radiology is now integrated in close relation with computer aided diagnostics, targeted interventional procedures and image guided minimally invasive surgeries. Computer enhanced reporting, where radiologists describe images by means of a structured notation for abnormal image features supplemented by a computer generated diagnosis, has been shown to improve the diagnostic accuracy of the general radiologist to equal that of specialists [1]. Radiological expertise is based on two kinds of skill: the swift and accurate processing of the normal appearance, and the ability to distinguish disease from normal variation in appearance [1]. The diagnostic quality of radiological image is increased if there is a better contrast between pathological lesion and the normal surrounding tissue.

From 2 to 3-dimensional imaging (e.g. coronal reformatting in computed tomography (CT) or perpendicular sequences in MRI) presenting the volumetric data of patients, post processing has evolved through dramatic changes and is now commonly used in diagnostic radiology. Advancement is 3D visualization of the imaging data sets where e.g. volume rendering techniques illustrate the anatomical structures as real on the screen and hence could further increase the diagnostic quality.

Radiology is also progressing from morphological to functional imaging. Recently, with the advancement of functional imaging, an additional dimension is added into the course of diagnostic and therapeutic monitoring. In order to integrate a fourth dimension into the conventional three dimensional visualization color mapping is one of the commonest methods used. The color map could be a representative time scale for dynamic contrast enhanced imaging [2], ventilation map for seeing the functionality of the lung [3] or even pre and post treatment image to evaluate the treatment success [4–6].

Although, gray scale display is still the gold standard for diagnostic imaging, color display systems are rarely found even in frontier research institutes. The real usefulness of color mapping in presenting the hidden data from usual gray scale images is unclear in particular for dynamic contrast enhanced MRI (DCE-MRI). Therefore, we intended to assess the value of color coded and gray-scale information from functional data with respect to diagnostic quality and accuracy (tumor vasculature) in DCE-MRI. Eight experienced radiologists were asked to rate both the diagnostic quality and tumor vasculature display on a series of gray-scale and model-based color coded images, from the same patients. It was also of interest whether there is a greater agreement between the observers in one image modality over another. To assess diagnostic accuracy of each image modality, the rating given for tumor vasculature display will be correlated with results from a quantitative region of interest (ROI) analysis. The ROI analysis will be calculated from the DCE-MRI data, where an increase in signal amplitude corresponds to increased vasculature in the tumor as previously demonstrated.

Materials and methods

Patients and diagnostic evaluation

A total of 19 patients (17 male, 2 female, age range 53–77 years, mean = 62.5 years) were diagnosed with a stage II ($n = 9$) and IV ($n = 10$) malignant pleuramesothelioma (MPM) and subsequently included in a prospective clinical study with single agent chemotherapy. The study protocol was approved by the institutional review board (IRB) and was according to the good clinical practice. Written informed consent was obtained from all patients after the procedure was fully explained to the patients. DCE-MRI was performed prior to therapy ($n = 19$), after the third ($n = 12$) and sixth ($n = 7$) cycle of chemotherapy. Seven patients (stage IV) did not participate in further imaging studies due to deterioration of their physical status. One patient died and four patients were lost during follow up for unknown reasons. All other patients underwent chemotherapy with Gemcitabine (2',2'-Difluorodesoxycytidin; Gemzar®, Lilly, Germany) in recommended dosage (1, 250 mg/m^2) and time period (six cycles) [7]. All patients underwent a pre-treatment pleural biopsy, which was evaluated with immuno-histopathology [8]. Tumors were staged and classified according to the WHO/UICC staging criteria and Butchart-MPM-Histopathologic Classification [9].

Magnetic resonance imaging and data post processing

Dynamic contrast enhanced magnetic resonance imaging (DCE-MRI) was performed using a 1.5 tesla MR clinical scanner (Siemens, Erlangen, Germany) with a T1-weighted 2D gradient echo sequence (repetition time (TR) 7.0ms, echo time (TE) 3.9 ms, matrix 256 ×

256, bandwidth: 260 Hz/s, 15 axial slices, 22 sequential repetitions) with a total acquisition time of approximately 9.86 min. Gadolinium-DTPA (Magnevist®, Schering AG, Germany) was administrated by slow injection rate (0.6ml/s of 0.1 mmol/kg bodyweight) after the third repetition using a power injector. Images were acquired during shallow respiration. Gray-scale images were produced by subtracting the first image from the last of the DCE-MRI series (Fig. 1a). DCE-MRI data (Fig. 1b) were post processed using a pharmacokinetic two compartment model on a Windows-based personal computer as previously described [10,11]. In-house software, which incorporates pharmacokinetic model [11], was used to place a region of interest at the point of maximum tumor width. On this slice the ROI was defined as the entire tumor (total tumor ROI). The resulting measure of maximum signal intensity (amplitude [a.u.]) was used as a measure of accuracy with respect to tumor vasculature. Color code reflecting pharmacokinetic parameters (Amp, k_{ep}) were generated. Based on the color maps, regions of interest (ROI) were created and evaluated for the whole tumor. In total 76 images were post processed (38 gray-scale and 38 color-coded images), while 6 images could not be converted adequately into the reading environment due to poor data acquisition, and therefore the final reading was confined to 70 images.

Reading

After anonymizing and post processing of the DCE-MRI data sets, data were uploaded to an internet server and personal login and passwords were sent to all the readers. The readings were performed on a personal computer (TFT screen 19 in.) with direct access to the internet using Microsoft Internet Explorer (v6.0, Microsoft®, USA). The readings were structured in ‘test read’ and ‘reading’. The test reading contained ten datasets to adapt the readers to the reading environment. Directly after the test readings, the readings of 70 images were started. Eight experienced radiologists, with a experience of more than 5 years each, were asked in a randomized fashion to rate all gray-scale and color map images for ‘diagnostic value’ and ‘tumor vasculature display’. For rating the image, a scale from −5 to +5 (−5 very poor and +5 excellent) was provided in the image with minimum interval of 0.25. The questions of ‘diagnostic value’ and ‘tumor vasculature’ were asked in a randomized fashion to all the raters regarding these 70 images.

Statistics and analysis

Statistical analysis and graphic visualization were performed with SigmaPlot (Systat Software Inc®, San Jose, CA, USA). To determine which technique was rated better for diagnostic quality, the rater scores of diagnostic quality for both techniques (gray scale and color coded) were compared using the Wilcoxon signed-rank test.

Furthermore, to assess tumor vascular display score, the rater scores of tumor vasculature for both techniques (gray scale and color coded) were also compared using the Wilcoxon signed-rank test.

Validity of the tumor vasculature display scores was assessed by correlating with the maximum amplitude of the total-tumor-region of interest (TT-ROI) analysis (score closer to the actual tumor microcirculation) [12], Spearman’s rank correlation coefficient was used

to assess the accuracy of visual and qualitative tumor vasculature by correlating ROI and rater score for both techniques over both the raters.

Intra-rater agreement for gray and color coded image was calculated for all the raters. Inter-rater agreement (Cohen's kappa coefficient) was also calculated for all the raters for gray and color images separately.

Results

All acquired and post-processed data was successfully uploaded on the server. All the raters scored all the 70 images according to their prepared randomized fashion. Overall scoring time was approximately 55 min for all the raters.

Scores of the raters for image diagnostic quality, was significantly lower for gray-scale images than color-coded images display ($p < 0.001$ for all raters). Median of gray-scale (−1 to 2.5) and color-coded (−1 to 4.5) image score for raters are shown in Table 1.

Scores for tumor vasculature were also assessed for the raters over both techniques. Scores for color-coded images display were found to be higher than gray-scale image scores ($p < 0.005$). Median of gray-scale (1–3.75) and color-coded (2–4) image score for raters are shown in Table 2.

ROI analysis (signal amplitude) and tumor vasculature display rater scores were correlated better with color-coded image compared to gray-scale images for all the raters. Significantly higher correlation coefficients were observed for color-coded images. Correlation coefficients for ROI signal amplitude with gray-scale and color-coded image scores for raters are shown in Fig. 2.

Intra-rater agreement between gray and color-coded images for diagnostic quality (mean 0.035) and tumor vascularity (mean 0.039)

Inter-rater agreement for gray and color image scorings among the raters were also calculated for diagnostic quality and tumor vascularity separately. The interrater agreement kappa value for diagnostic quality for gray and color coded images are 0.075 and 0.049, respectively. Kappa value for tumor vascularity for gray and color coded images are 0.073 and 0.075, respectively.

ROC analysis was done for tumor vascularity score for gray and color-coded images with respect to tumor amplitude score for all the raters shown in Fig. 3.

Discussion

Our results showed lower rater scores for gray-scale than color map images for image diagnostic quality. Furthermore, average rater score of tumor vascular display was significantly higher for color images and also correlated significantly with total-tumor-ROI amplitude analysis, which was considered directly related to actual tumor microcirculation.

Oncologic radiology has been an essential part of magnetic resonance imaging and has evolved tremendously in the last two decades. The basis of oncologic imaging is to depict the morphologic description of the pathological lesions. The diagnostic quality of images is enhanced manifolds by 3D volumetric imaging (e.g. coronal reformatting in computed tomography (CT) or perpendicular sequences in MRI) data sets.With the advancement of multi-detector CT and fast MR sequences, high resolution anatomical imaging can be performed efficiently in the clinical environment. Static imaging in oncology provides information only with respect to structural changes over time, which becomes apparent much later than functional changes in metabolic or microcirculatory rates. Some therapies such as anti-angiogenics and vaccines are expected to be cytostatic and thus do not produce “objective” or measurable response in tumor size [13]. Therefore, methods of measuring functional changes in the tumor would be beneficial to predict the therapeutic value of the drug in these circumstances. Radiology is thus progressing from morphological imaging to functional imaging.

With the functional characteristics in the image, an additional fourth dimension is added into the imaging course. The fourth dimension can be a time scale for perfusion imaging [2], ventilation map for lung [3] or even pre and post-treatment image to confirm the treatment success [4–6]. Color mapping is used to illustrate the fourth dimension on the conventional three dimensional gray-scale imaging. With advanced color coded display systems, interpretation of functional data becomes more attractive as functional data can be visualized in a detailed fashion. With technologically advanced workstations to post-process the data and higher screen resolution, color visualization of functional data becomes a real possibility in the clinical environment.

It has been proved that color digital summation radiography is having better diagnostic quality over gray-scale imaging subtraction technique in a study by Ogata et al. [14]. It has not yet been established, however, whether viewing functional images in color has any advantages over gray-scale images in DCE-MRI, which is in common clinical use. Therefore, we intend to assess the value of color and gray-scale information from functional data with respect to diagnostic quality and tumor vasculature display accuracy in DCE-MRI.

Dynamic contrast enhanced magnetic resonance imaging (DCE-MRI) studies produces time series images that enable pixel by pixel analysis of contrast kinetics within a tumor [11]. These time-signal curves can be analyzed with descriptive heuristic tools, such as initial slope, time to peak or rate of washout [15]. The value of dynamic contrast enhanced MRI has been demonstrated for many different tumors [16–19]. Such methods are easy to apply and reflect the functional aspects of the tumor for both diagnosis and therapeutic interventions [16]. Advantageously, this technique can be performed in most clinical MRI systems equipped with standard coils and an automated injectors [16]. DCE-MRI involves sequential acquisition of images during intra-venous administration of a gadolinium chelate. The temporal passage of contrast media through tissue, including neoplastic (neoangiogenic) tissue, reflects its microcirculation (vasculature) and can be used to assess and map out differences in microcirculation and vascular permeability [5].

The assessment of contrast arrival was done by either subtraction methods or DCE-MRI sequencing. In subtraction method T1 weighted pre-contrast image are subtracted from the T1 weight post-contrast image and the results is evaluated as the parameter of functional change in the lesion. Whereas, dynamic technique depict pre-contrast, dynamic and post-contrast phases [16] in a sequence. All these modalities were mainly based on gray-scale display systems. It is good to visualize the differentiation between areas which vary widely in gray-scale values in gray-scale display systems, but not for closely variable regions. Further disadvantage in gray-scale display technique was, imaging of moving chest organs like lungs and breasts. These images produce motion artefacts in the subtraction technique, which appear as pseudo-enhancement pattern. Fat suppression technique is a good alternative used in breast MRI to surmount this problem [20], but it is still time consuming. Color-coded imaging technique helps overcome these limitations and is now coming in regular clinical use. In conventional radiography both signal and background are displayed in gray scale, so signal can be difficult to recognize at low contrast. However, in color display, signal is color coded and displayed on gray scale background image. So even the slightest change in signal can be displayed with different color and will be easily distinguished with naked eyes. Human eyes are perceptible to color differentiation over a wide range to have a better contrast.

Therefore, color coded imaging are more informative as even the faint changes are easily distinguished and it expands the contrast between normal and pathological tissue over a wider range as suggested by human eye physiology.

Conclusion

Visual perception of color coded imaging correlates well with actual pathological changes. Color coded imaging is also more informative than conventional gray-scale imaging as it expands the contrast between normal and pathologically diseased tissues, its use in clinical studies should be encouraged. Color imaging hold promising future for computer assisted diagnostics and interventional radiology.

Abbreviations

Amp
Amplitude (a.u.)

DCE-MRI
Dynamic contrast enhanced magnetic resonance imaging

k_{el}
Elimination rate constant (min^{-1})

k_{ep}
Redistribution rate constant (min^{-1})

ROI
Region of interest

TT-ROI

Total-tumor-region of interest

References

1. Sharples M, Jeffery NP, du Boulay B, Teather BA, Teather D, du Boulay GH (2000) Structured computer-based training in the interpretation of neuroradiological images. Int J Med Inform 60:263–280. doi:10.1016/S1386-5056(00)00101-5 [PubMed: 11137471]
2. Fuss M, Wenz F, Scholdei Ret al.(2000)Radiation-inducedregional cerebral blood volume (rCBV) changes in normal brain and low-grade astrocytomas: quantification and time and dose-dependent occurrence.Int J Radiat Oncol Biol Phys48:53–58. doi:10.1016/S0360-3016(00)00590-3 [PubMed: 10924971]
3. Fink C, Ley S, Risse Fet al. (2005) Effect of inspiratory and expiratory breathhold on pulmonary perfusion: assessment by pulmonary perfusion magnetic resonance imaging. Invest Radiol 40:72–79. doi:10.1097/01.rli.0000149252.42679.78 [PubMed: 15654250]
4. Kiessling F, Huber PE, Grobholz Ret al. (2004) Dynamic magnetic resonance tomography and proton magnetic resonance spectroscopy of prostate cancers in rats treated by radiotherapy. Invest Radiol 39:34–44. doi:10.1097/01.rli.0000095472.37056.0b [PubMed: 14701987]
5. Giesel FL, Bischoff H, von Tengg-Kobligk Het al. (2006) Dynamic contrast-enhanced MRI of malignant pleural mesothelioma: a feasibility study of noninvasive assessment, therapeutic follow-up, and possible predictor of improved outcome. Chest 129:1570–1576. doi:10.1378/chest.129.6.1570 [PubMed: 16778277]
6. Hayes C, Padhani AR, Leach MO (2002) Assessing changes in tumour vascular function using dynamic contrast-enhanced magnetic resonance imaging. NMR Biomed 15:154–163. doi:10.1002/nbm.756 [PubMed: 11870911]
7. Kroep JR, Peters GJ, van Moorsel CJet al. (1999) Gemcitabine-cisplatin: a schedule finding study. Ann Oncol 10:1503–1510. doi:10.1023/A:1008339425708 [PubMed: 10643544]
8. Kayser K, Bohm G, Blum Set al. (2001) Glyco- and immunohistochemical refinement of the differential diagnosis between mesothelioma and metastatic carcinoma and survival analysis of patients. J Pathol 193:175–180. doi:10.1002/1096-9896(2000)9999:9999<::AID-PATH772>3.0.CO;2-T [PubMed: 11180163]
9. Butchart EG, Ashcroft T, Barnsley WC, Holden MP (1976) Pleuropneumonectomy in the management of diffuse malignant mesothelioma of the pleura. Experience with 29 patients. Thorax 31:15–24. doi:10.1136/thx.31.1.15 [PubMed: 1257933]
10. Knopp MV, von Tengg-Kobligk H, Choyke PL (2003) Functional magnetic resonance imaging in oncology for diagnosis and therapy monitoring. Mol Cancer Ther 2: 419–426 [PubMed: 12700286]
11. Brix G, Semmler W, Port R, Schad LR, Layer G, Lorenz WJ (1991) Pharmacokinetic parameters in CNS Gd-DTPA enhanced MR imaging. J Comput Assist Tomogr 15:621–628. doi:10.1097/00004728-199107000-00018 [PubMed: 2061479]
12. Giesel FL, Choyke PL, Mehndiratta Aet al. (2008) Pharmacokinetic analysis of malignant pleural mesothelioma-initial results of tumor microcirculation and its correlation to microvessel density (CD-34). Acad Radiol 15:563–570. doi:10.1016/j.acra.2007.12.014 [PubMed: 18423312]
13. Folkman J (1995) Seminars in Medicine of the Beth Israel Hospital, Boston. Clinical applications of research on angiogenesis. N Engl J Med 333:1757–1763. doi:10.1056/NEJM199512283332608 [PubMed: 7491141]
14. Ogata Y, Naito H, Azuma Het al. (2006) Novel display technique for reference images for visibility of temporal change on radio-graphs–color digital summation radiography. Radiat Med 24:28–34. doi:10.1007/BF02489986 [PubMed: 16715659]
15. Padhani AR, Husband JE (2001) Dynamic contrast-enhanced MRI studies in oncology with an emphasis on quantification, validation and human studies. Clin Radiol 56:607–620.doi:10.1053/crad.2001.0762 [PubMed: 11467863]

16. Knopp MV, Giesel FL, Marcos H, von Tengg-Kobligk H, Choyke P (2001) Dynamic contrast-enhanced magnetic resonance imaging in oncology. Top Magn Reson Imaging 12:301–308. doi:10.1097/00002142-200108000-00006 [PubMed: 11687716]

17. Kuhl CK, Mielcareck P, Klaschik Set al. (1999) Dynamic breast MR imaging: are signal intensity time course data useful for differential diagnosis of enhancing lesions?. Radiology 211: 101–110 [PubMed: 10189459]

18. Weidner N, Semple JP, Welch WR, Folkman J (1991) Tumor angiogenesis and metastasis—correlation in invasive breast carcinoma. N Engl J Med 324: 1–8

19. Fletcher BD, Hanna SL, Fairclough DL, Gronemeyer SA (1992) Pediatric musculoskeletal tumors: use of dynamic, contrast-enhanced MR imaging to monitor response to chemotherapy. Radiology 184: 243–248 [PubMed: 1319075]

20. Gilles R, Guinebretiere JM, Shapeero LGet al. (1993) Assessment of breast cancer recurrence with contrast-enhanced subtraction MR imaging: preliminary results in 26 patients. Radiology 188: 473–478 [PubMed: 8327700]

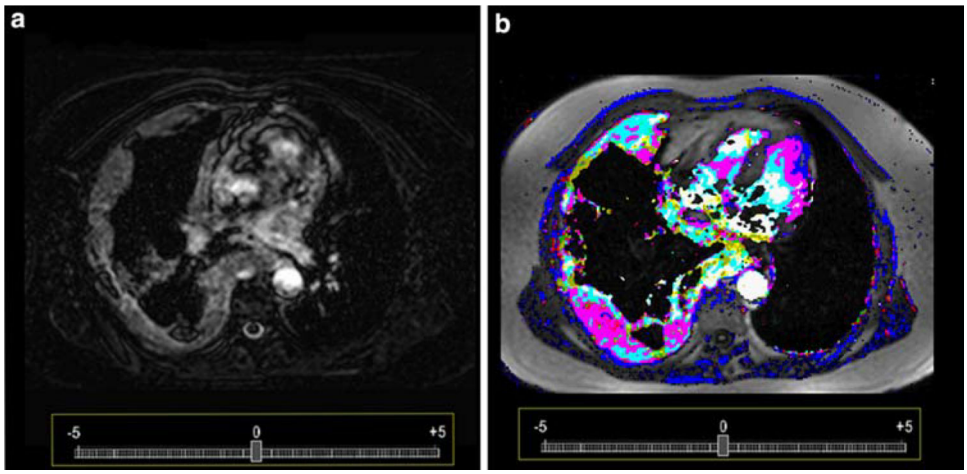

Fig. 1.

Subtraction images (**a**) presenting a patient with malignant pleural mesothelioma adjacent to the right chest wall. The high masculinity of the tumor can be already appreciated to most of the tumor tissue. Color code display (**b**) presents the same tumor vasculature as in **a**, but on the basis of a post processed dynamic contrast enhanced MRI. Tumor vasculature is better visualized and hyper- and hypo-vascular areas can be well differentiated

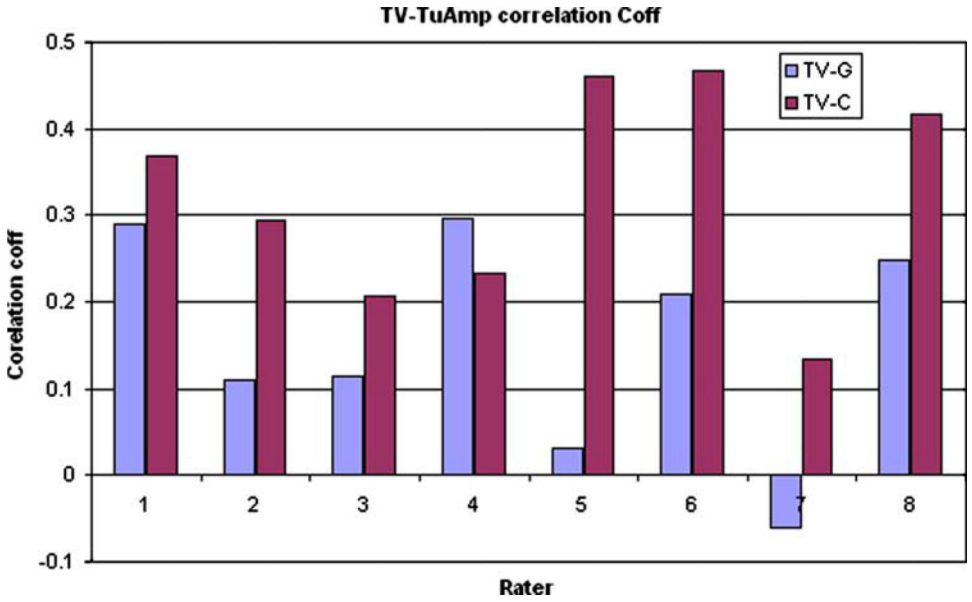

Fig. 2.

Spearman's rank correlation coefficients for tumor vascularity with signal drop amplitude for the eight rates

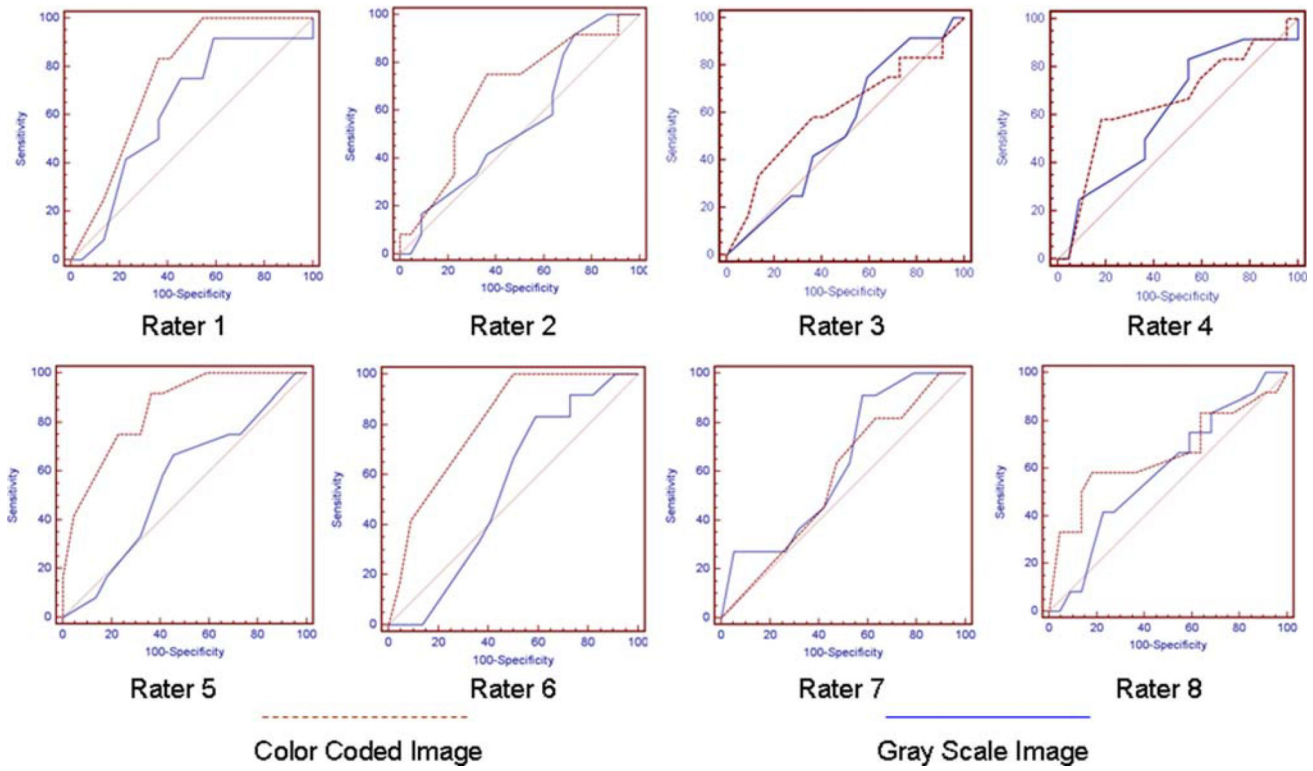

Fig. 3.
ROC analysis for tumor vascularity with gray scale and color coded images for eight raters

Table 1

Median of gray scale (−1 to 2.5) and color coded (−1 to 4.5) image score of raters for diagnostic quality

Rater	Median gray image score for diagnostic quality	Median color image score for diagnostic quality
1	2.50	4.00
2	2	4
3	1	4.5
4	−1	−1
5	2	3
6	1	4
7	1.5	4
8	0.75	4.5

Table 2

Median of gray scale (1–3.75) and color coded (2–4) image score of raters for tumor vascularity

Rater	Median gray image score for tumor vascularity	Median color image score for tumor vascularity
1	2.00	4.00
2	2	2.75
3	3.75	3
4	1	3
5	2.5	2
6	2	4
7	1	3.5
8	1	2